PB87-193546

# Continuous Stirred Tank Reactor Investigation of the Gas-Phase Reaction of Hydroxyl Radicals and Toluene

(U.S.) Environmental Protection Agency
Research Triangle Park, NC

1985

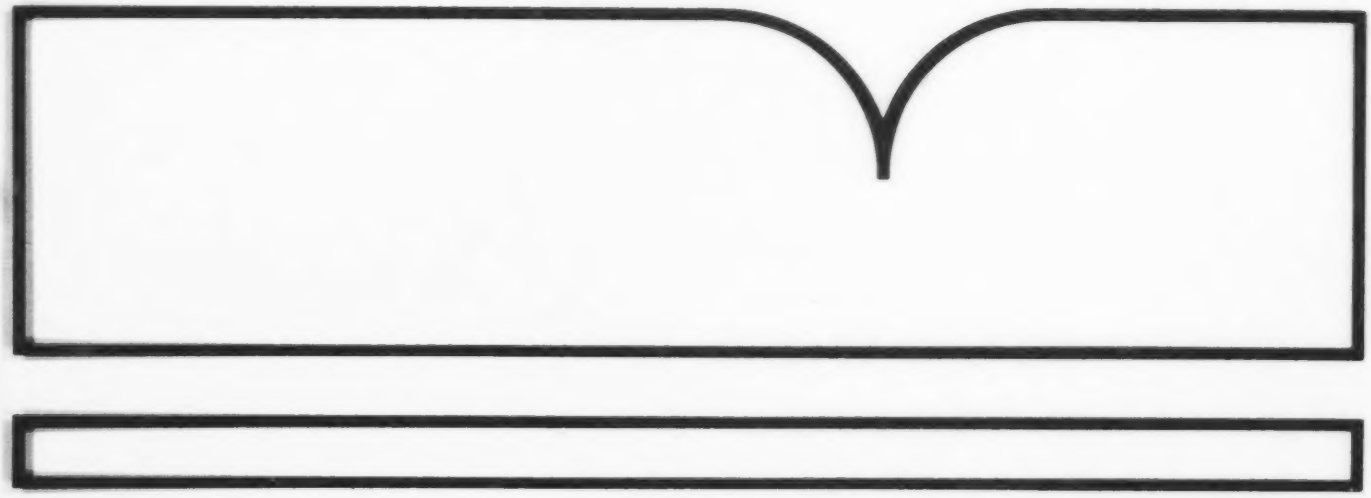

U.S. Department of Commerce
National Technical Information Service
NTIS

**TECHNICAL REPORT DATA**
*(Please read Instructions on the reverse before comp'*

| 1. REPORT NO. | 2. | PB87-193546 |
|---|---|---|
| EPA/600/J-85/487 | | |

| 4. TITLE AND SUBTITLE | 5. REPORT DATE |
|---|---|
| A CONTINUOUS STIRRED TANK REACTOR INVESTIGATION OF THE GAS-PHASE REACTION OF HYDROXYL RADICALS AND TOLUENE (Journal Version) | 1985 |
| | 6. PERFORMING ORGANIZATION CODE |
| 7. AUTHOR(S) | 8. PERFORMING ORGANIZATION REPORT NO. |
| M.W. Gery, D.L., Fox, H.E. Jeffries, L. Stockburger and W.S. Weathers | |
| 9. PERFORMING ORGANIZATION NAME AND ADDRESS | 10. PROGRAM ELEMENT NO. |
| Dept. of Environmental Science and Engineering<br>University of North Carolina<br>School of Public Health<br>Chapel Hill, NC | CDTA1D/02-2153 (FY-85) |
| | 11. CONTRACT/GRANT NO. |
| | CR809954 |
| 12. SPONSORING AGENCY NAME AND ADDRESS | 13. TYPE OF REPORT AND PERIOD COVERED |
| Atmospheric Sciences Research Laboratory - RTP, NC<br>Office of Research and Development<br>U.S. Environmental Protection Agency<br>Research Triangle Park, N.C. 27711 | 14. SPONSORING AGENCY CODE<br>EPA/600/09 |

15. SUPPLEMENTARY NOTES

REF: Int. J. Chem. Kinet., 17:931-955, September 1985

16. ABSTRACT

A continuous stirred tank reactor (CSTR) was used to study the gas phase reaction between HO and toluene. HO was generated by the in situ photolysis of nitrous acid. Flow reactor operation at steady state conditions with a residence time of 20 minutes allowed investigation of primary and very rapid secondary reactions. CSTR and batch reactor experiments were also performed with selected products. Both gas phase and aerosol products were identified by chromatography and mass spectroscopy, with total product yields between 55 and 75 percent of reacted carbon. Toluene reaction products included cresols, nitrocresols, nitrotoluenes, 3,5-dinitrotoluene, benzaldehyde, benzyl nitrate, nitrophenols, methyl-p-benzoquinone, methylglyoxal, glyoxal, formaldehyde, methyl nitrate, PAN and CO. The fraction of HO methyl hydrogen abstraction was calculated to be $0.13 \pm 0.04$. The ratio of reaction rate constants for nitrotoluene versus cresol formation from the HO adduct was calculated to be about $3.3 \times 10^4$. Also, the ratio of cresol formation versus $O_2$ addition to the HO adduct was estimated to be $\geq 0.55$. Comparisons of these measurements with previous values and the implications with respect to photochemical kinetics modeling of the atmosphere are discussed.

17. KEY WORDS AND DOCUMENT ANALYSIS

| a. DESCRIPTORS | b. IDENTIFIERS/OPEN ENDED TERMS | c. COSATI Field/Group |
|---|---|---|
| | | |

REPRODUCED BY
U.S. DEPARTMENT OF COMMERCE
NATIONAL TECHNICAL
INFORMATION SERVICE
SPRINGFIELD, VA 22161

| 18. DISTRIBUTION STATEMENT | 19. SECURITY CLASS (This Report) | 21. NO. OF PAGES |
|---|---|---|
| RELEASE TO PUBLIC | UNCLASSIFIED | 26 |
| | 20. SECURITY CLASS (This page) | 22. PRICE |
| | UNCLASSIFIED | |

EPA/600/J-85/487
JOURNAL ARTICLE

# A Continuous Stirred Tank Reactor Investigation of the Gas-Phase Reaction of Hydroxyl Radicals and Toluene

MICHAEL W. GERY,*† DONALD L. FOX, and HARVEY E. JEFFRIES

*Department of Environmental Sciences and Engineering, School of Public Health, University of North Carolina, Chapel Hill, North Carolina 27514*

LEONARD STOCKBURGER and WALTER S. WEATHERS

*Environmental Sciences Research Laboratory, United States Environmental Protection Agency, Research Triangle Park, North Carolina 27711*

## Abstract

A continuous stirred tank reactor (CSTR) was used to study the gas-phase reaction between HO· and toluene. HO· was generated by the *in situ* photolysis of nitrous acid. Flow reactor operation at steady-state conditions with a residence time of 20 min allowed investigation of primary and very rapid secondary reactions. CSTR and batch reactor experiments were also performed with selected products. Both gas-phase and aerosol products were identified by chromatography and mass spectroscopy, with total product yields between 55 and 75% of reacted carbon. Toluene reaction products included cresols, nitrocresols, nitrotoluenes, 3,5-dinitrotouluene, benzaldehyde, benzyl nitrate, nitrophenols, methyl-*p*-benzoquinone, glyoxal, methylglyoxal, formaldehyde, methyl nitrate, PAN, and CO. The fraction of HO· methyl hydrogen abstraction was calculated to be 0.13 ± 0.04. The ratio of reaction rate constants for nitrotoluene versus cresol formation from the HO·-adduct was calculated to be about $3.3 \times 10^4$. Also, the ratio of cresol formation versus $O_2$ addition to the HO·-adduct was estimated to be ≥0.5 for atmospheric conditions. Comparisons of these measurements with previous values and the implications with respect to photochemical kinetics modeling of the atmosphere are discussed.

## Introduction

Alkylbenzene species comprise a significant portion of the reactive hydrocarbon compounds in urban atmospheres [1,2]. Of these, toluene is often the most prevalent, since it occurs in automobile exhaust [3,4] and is used as an industrial solvent. Under conditions typical of photochemical smog, the major toluene oxidation reaction is with the hydroxyl radical (HO·) [5,6]. Reactions with ozone, atomic oxygen ($O^{3}P$), and $NO_3$ have been shown to be comparatively slow under ambient conditions [7–9]. Although the relative importance of these initial toluene reactions has been confirmed, much uncertainty remains

*To whom all correspondence should be addressed.
†Current address: Systems Applications, Inc., 101 Lusas Valley Rd., San Rafael, CA 94903.

International Journal of Chemical Kinetics, Vol. 17, 931–955 (1985)
© 1985 John Wiley & Sons, Inc. CCC 0538-8066/85/090931-25$04.00

in the description of the complete reaction process because experimental product yields have often been low.

Considerable effort has been spent determining the identity of HO·-toluene reaction products and discerning their further chemical reactions in the gas phase. Various product species containing aromatic rings have been detected, including benzaldehyde, cresols, nitrotoluenes, nitrocresols, nitrophenols, phenol, benzyl nitrate, and benzyl alcohol [10–20]. More recent discoveries of $\alpha$- and $\gamma$-dicarbonyl species seem to indicate that ring-fragmentation processes may be of greater importance than previously expected [20–25]. Although important reaction rates for a few stable intermediate species have been determined [9,26,27], the remaining uncertainty allows different photochemical kinetics models to treat HO·-alkylbenzene chemistry in a variety of ways [18,28–30].

One reason that HO·-alkylbenzene chemistry has remained elusive is that hydroxyl radicals are very reactive and their concentrations low (less than parts per trillion); hence, HO· is difficult and expensive to produce and monitor. In this work a continuous stirred tank reactor (CSTR) was chosen to take advantage of the distinctive temporal characteristics of a flow-type reactor. Operation of a CSTR at steady-state conditions and ambient temperatures and pressures minimizes many of the uncertainties that occur in temporally varying batch reactors and low-pressure chemical dynamics studies. Also, *in situ* creation of hydroxyl radical through the photolysis of nitrous acid (at ca. 310 to 390 nm),

$$\text{HONO} + h\nu \longrightarrow \text{HO}\cdot + \text{NO} \tag{1}$$

provides a constant concentration of HO· and minimizes any ozone formed through its reaction with NO.

## Experimental

### *Procedure*

Because CSTRs operate (ideally) under steady-state conditions, the description of mass balance is simple. After operation for about seven residence times, steady state is achieved, and mass balance may be described by [31]

$$R = ([C]_{out} - [C]_{in})/\tau, \tag{2}$$

where $\tau$ is the residence time ($\tau = v/f$, $V$ is CSTR volume, and $f$ is flow rate), $[C]_{in}$ and $[C]_{out}$ are constant inlet and outlet concentrations, and $R$ is the rate of reaction. The reactor used was designed to be operated at residence times of about 20 min. This value was chosen to allow the HO·-toluene reaction mixture to advance to rapidly occurring secondary reactions, but to decouple the system from long-term loss of less reactive products.

Continuous stirred tank reactors are useful not only for kinetics studies, but can also serve as product generators. Operating the system at steady state and sampling from the outlet provides a large product mass without altering the chemical conditions producing the product. Thus, trace products and highly reactive species can accumulate to identifiable portions. Also, quantification of major product yields is more precise. In this study, XAD-2 gas-phase samples and quartz-fiber aerosol filters were collected and extracted for subsequent gas chromatographic-mass spectral (GCMS), gas chromatographic (GC), and high-pressure liquid chromatographic (HPLC) analyses.

The CSTR was generally operated as a flow reactor. A set of batch experiments, however, were performed under HONO/$h\nu$ conditions similar to those of the flowing system to find which secondary products derived from identified, primary products. In both flow and batch experiments, blank chamber, dark HONO, dark hydrocarbon/HONO, and hydrocarbon/$h\nu$ samples were analyzed to investigate background or interference responses.

*Apparatus*

The CSTR consists of a Teflon®-coated, cylindrical, steel frame surrounded by 5-mil FEP Teflon film with a volume of ca. 200 L. By varying throughput flow rates between 25 and 4 L/min, residence times can be varied between 8 and 50 min. The reaction chamber is surrounded by 34 UV fluorescent (GE, F20 BLB) lamps mounted on a reflective surface. Maximum light intensity, as $NO_2$ photolysis rate, is approximately 0.30 $min^{-1}$. A diagram of the flow system is shown in Figure 1. Flow through the CSTR is provided by a downstream vacuum pump and an upstream source of pressurized carrier gas. Balancing these flows maintains the CSTR at atmospheric pressure throughout an experiment.

Nitrous acid was generated by the liquid-phase reaction of sodium nitrite with sulfuric acid. HONO, NO, and $NO_2$ were offgassed as products of this reaction. The technique and apparatus used for HONO generation was a composite of previously described reactors [10,32–34]. Dry nitrogen was passed through a bank of three parallel HONO generating flasks and a mixing bulb prior to CSTR input. The HONO flux out of the equilibrating flask was allowed to stabilize prior to use as input to the CSTR. The average operating range for the ratio of HONO to total generated $NO_x$ was 15 to 30%. It was found that production of greater amounts of HONO leads to undesirably high $NO_2$ concentrations.

*Instrumentation*

Toluene was monitored every 4 min by a GC with flame-ionization detector (FID) and a 50.8 cm × 1.6 mm I.D. stainless-steel column

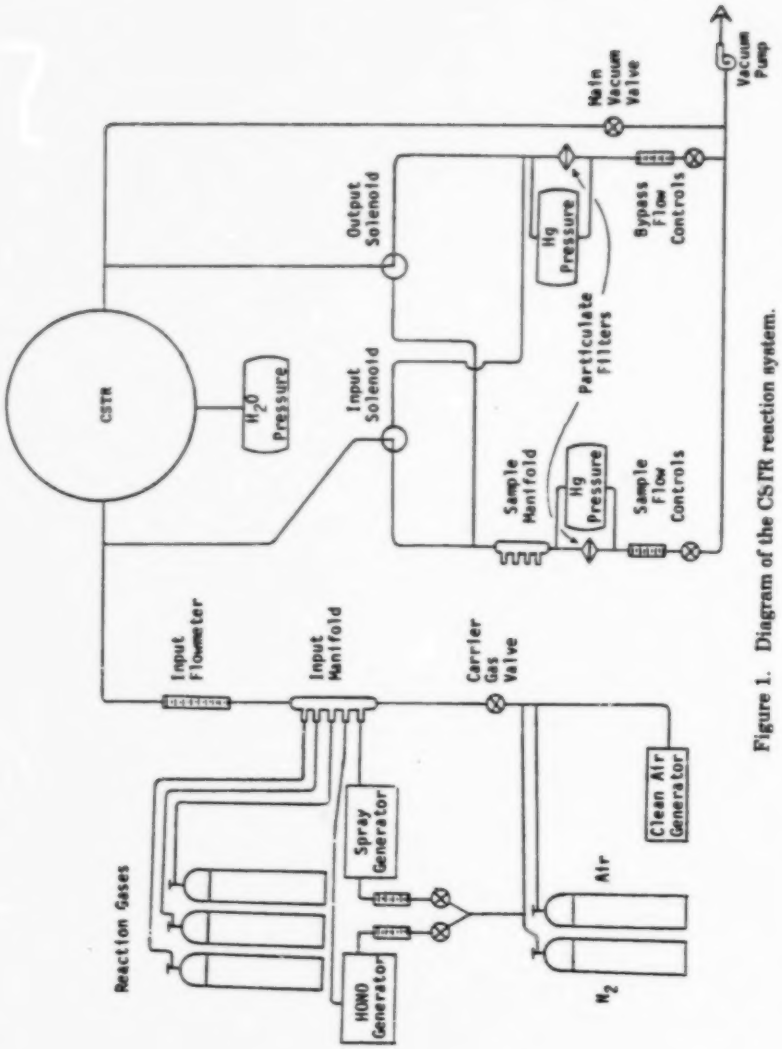


Figure 1. Diagram of the CSTR reaction system.

packed with 10% TCEP on 100/120 mesh Chromasorb PAW. Aromatic products were concentrated at −77°C in an 11-$cm^3$ trap packed with 40-$\mu$m glass beads, then electrically heated and injected to a 30-m × 0.25-mm DB1 capillary column and FID. A GC with an electron capture detector was used to monitor PAN, methylglyoxal, and organic nitrites with a 1.2-m × 1.6-mm glass column packed of 10% Carbowax 600 on 60/80 mesh Gas Chrom Z operated at 25°C with Argon/Methane carrier gas.

Glyoxal and methylglyoxal were collected with a bubbler containing an absorbing reagent of acidified 2,4-dinitrophenylhydrazine (DNPH) [35]. Analysis was performed by HPLC of the dicarbonyl-DNPH derivatives [36] with a MCH-10 reverse phase, 30-cm × 9-mm column and a fixed 254-nm detector. XAD-2 resin and quartz-fiber filters were used to collect gas and aerosol-phase samples for later analysis. Both were extracted with methylene chloride and concentrated. Qualitative analysis was performed by a HP-5992 GCMS system and by a second GC equipped with both a flame-ionization detector and a thermionic-specific detector.

A Bendix 8101-B chemiluminescent $NO_x$ analyzer was used in the NO-only mode as the oxides of nitrogen sensor. Although NO and total $NO_x$ are relatively easy to measure, intermediate oxidation states such as $NO_2$ and HONO must be selectively separated from the other species and calculated by difference in the $NO_x$ signal. Methods of separation for nitrogen oxides and oyxacids were initially described by Cox [32] and later utilized and confirmed by Hoshino, Akimoto, and Okuda [10]. Ozone was monitored by a Bendix 8002 series chemiluminescent analyzer. Because of the high NO concentration in the reactor, only traces of $O_3$ were detected. A Beckman 6800 gas chromatograph was used to monitor carbon monoxide. Formaldehyde was analyzed with a CEA Instruments, Inc., 555 colorimetric analyzer [37].

### *Materials*

A compressed-gas cylinder of toluene in nitrogen was used for continuous hydrocarbon injection. Both it and a calibration cylinder of toluene in nitrogen were obtained from Scott Specialty Gases. Other reagents and calibration species were obtained from Aldrich Chemical Co. and Phaltz and Bauer, Inc. An AADCO clean-air generator or cylinders of compressed nitrogen were used to deliver dry carrier gas.

## Results

Seven toluene CSTR experiments were performed with HONO and light. To supplement the information from the toluene CSTR systems, the chemistry of some major products was studied. In the case of

benzaldehyde, it was possible to create a high concentration source of injection vapor; and thus, CSTR tests were performed. Two benzaldehyde photolysis and two benzaldehyde/HONO/$h\nu$ experiments were conducted. To investigate the possible relationships between apparent primary products and suspected secondary species, the CSTR was operated in batch mode for HONO/$h\nu$ systems of *o*-, *m*-, and *p*-cresol, *m*-nitrotoluene, and methyl-*p*-benzoquinone. The methyl-*p*-benzoquinone photolysis system was also studied in this manner. In addition to real-time analysis, XAD-2 cartridge and aerosol filter samples were collected for three toluene/HONO/$h\nu$, one benzaldehyde/$h\nu$, and two benzaldehyde/HONO/$h\nu$ CSTR experiments. XAD-2 cartridge samples were collected for all batch systems. They were analyzed later by both GC and GCMS.

A summary of the toluene/HONO/$h\nu$ experimental data is given in Table I. The top portion of Table I contains information describing the conditions of each experiment, and the remainder contains product percent (of reacted carbon) yields. Experiments are ranked in order of residence times. Although acetone, acrolein, and higher aliphatic aldehydes, including acetaldehyde, could have been detected, none were found. In addition, conjugated $\gamma$-dicarbonyl species were not detected with the HPLC. PAN was always measured at low concentrations, perhaps because thermal decomposition could have been significant at the experimental conditions. Minor amounts of methyl nitrate and formic acid may have been present, but they were not quantified. Conspicuously absent in all real-time analyses of higher-molecular-weight products were phenol and benzyl alcohol.

Table II shows aerosol yields from three toluene/HONO/$h\nu$ experiments. Three nitro-*o*-cresol species were detected in the filter extracts, two of which were also measured in the gas phase (3-nitro- and 5-nitro-2-hydroxytoluene). The third isomer, 4-nitro-2-hydroxytoluene, was not measured in the gas-phase XAD-2 extractions of either the toluene experiments or the *o*-cresol batch experiment. One nitro-*p*-cresol species (3-nitro-4-hydroxtoluene) was detected in both the batch and CSTR experiments. It occurred in both gas and aerosol samples, although the condensed yield was small. Both *m*- and *p*-nitrotoluene were detected in the toluene CSTR experiments, along with significant amounts of 3,5-dinitrotoluene.

Four benzaldehyde photolysis experiments with residence times of approximately 21 min were performed in the CSTR: two with HONO and two without. Two high-molecular-weight gas-phase products were monitored during the HONO photolysis experiments. The higher concentration species was identified as *o*-nitrophenol (in yields of 14.6 and 12.5% of reacted benzaldehyde); the second species was not identified (estimated 2.6 and 3.9% yields). Benzoic acid may also be an oxidation product, but the amount detected in the extraction

TABLE I. Product distributions for toluene CSTR experiments (units are ppmC unless given).

| | Conditions | | | | | | |
|---|---|---|---|---|---|---|---|
| Experiment Number | 1 | 2 | 3 | 4 | 5[e] | 6 | 7 |
| Residence Time (min.) | 8.35 | 12.51 | 18.35 | 21.45 | 21.47 | 22.08 | 22.66 |
| Dark exit concentration (ppmC) | 166.80 | 87.95 | 171.09 | 87.95 | 116.68[c] | 111.05 | 99.41 |
| Lights-on exit concentration (ppmC) | 165.33 | 83.12 | 159.32 | 82.51 | 108.31 | 102.97 | 91.78 |
| Δ[toluene] (ppmC) | 3.47 | 4.83 | 11.77 | 5.44 | 8.37[c] | 8.08 | 7.63 |
| Δ[toluene] (percent) | 2.06 | 5.49 | 6.88 | 6.19 | 6.15[c] | 7.28 | 7.68 |
| Inlet $[NO_x]$ (ppm) | n.a. | 4.5 | 19.3 | 6.6 | 20.1 | 10[e] | 9.4 |
| $[HC]/[NO_x]$ (ppmC/ppm) | n.a. | 19.5 | 8.9 | 13.3 | 5.8[c] | 11.1[e] | 15.5 |
| Chamber Temperature (Kelvin) | 301.5 | 303.1 | 308.7 | 306.2 | 305.9 | 303.0 | 302.8 |
| | Product Distribution (Percent of Reacted Carbon) | | | | | | |
| Carbon Monoxide | 2.6 | 2.7 | n.a. | 4.2 | 2.5 | 2.2 | 3.9 |
| Formaldehyde | n.a. | 1.3 | n.a. | n.a. | 1.3 | 1.5 | 1.4 |
| Glyoxal | 4.3 | 2.7 | 3.4 | 2.6 | 1.4 | 1.4 | 2.1 |
| Methylglyoxal | 5.6 | 4.8 | 6.0 | 3.7 | 2.2 | 2.0 | 3.3 |
| Peroxyacetylnitrate | 0.6 | 0.2 | 0.2 | 0.4 | n.a. | 0.3 | 0.1 |
| Benzyl Nitrate | 1.4 | 1.0 | 0.4 | 1.0 | | 0.8 | 1.3 |
| Benzaldehyde | 16.6 | 9.1 | 10.5 | 11.3 | | 9.9 | 9.8 |
| o-Nitrophenol | tr. | 0.0 | 0.6 | 0.0 | | 0.6 | tr. |
| o-Nitrotoluene | 1.4 | 0.9 | 0.5 | 0.7 | | 0.6 | 0.7 |
| m-Nitrotoluene | 10.5 | 6.5 | 6.1 | 8.0 | | 4.5 | 6.4 |
| p-Nitrotoluene | 3.6 | 2.5 | 1.4 | 2.4 | | 1.4 | 2.2 |
| Methyl-p-benzoquinone | 5.5 | 4.0 | 4.7 | 4.0 | | 4.7 | 3.7 |
| o-Cresols: | | | | | | | |
| o-Cresol | 4.4 | 5.4 | 5.8 | 6.2 | | 4.9 | 5.1 |
| 3-Nitro-2-hydroxytoluene | 15.1 | 10.9 | 6.4 | 9.3 | | 7.4 | 11.0 |
| 5-Nitro-2-hydroxytoluene | 9.9 | 7.1 | 6.3 | 6.1 | | 4.9 | 7.2 |
| m- and p-Cresols: | | | | | | | |
| m- and p-Cresol | 3.3 | 1.4 | 0.4 | 1.1 | | 0.9 | 1.2 |
| 3-Nitro-4-hydroxytoluene | 6.7 | 3.9 | 3.3 | 3.1 | | 3.4 | 3.6 |
| Unidentified Gas Phase Species (approx.) | 9.2 | 1.6 | 1.5 | 1.5 | | 2.2 | 1.2 |
| Aerosol | 1.4 | 6.2 | n.a. | 4.2 | | 4.7 | 5.1 |
| Percent of Reacted Carbon Detected | 104.6[b,c] | 72.2 | 57.5[e] | 69.5[e] | | 58.5 | 69.3 |

[n.a.] = Data not available.

[tr.] = Trace amount detected.

[a] Gas chromatograph calibrations not available for this experiment. Data not included in table.

[b] Total reacted carbon value is low because some instruments were not operating on this day.

[c] This value has a large associated error because the denominator, Δ[toluene], had low measurement precision.

[e] Estimated.

TABLE II. Product distributions for methylene chloride extractions of toluene filters

| | Conditions | | | |
|---|---|---|---|---|
| Experiment | 1 | 2 | 6 | |
| Total Weight (μg) | 182 | 178 | 298 | |
| Sample Time (min.) | 133 | 83 | 131 | |
| Volume of Air Sampled ($m^3$) | 2.8 | 1.1 | 0.8 | |
| Concentration ($\mu g/m^3$) | 1.1 | 4.0 | 9.1 | |
| | Product Distribution (Percent of Aerosol Carbon) | | | Average |
| m-Nitrotoluenes: | | | | |
| m-Nitrotoluene | 0 | 6 | 22 | 9.3 |
| 3,5-Dinitrotoluene | 7 | 10 | 16 | 11.0 |
| p-Nitrotoluene | 0 | 0 | 3 | 1.0 |
| o-Cresols: | | | | |
| 3-Nitro-2-hydroxytoluene | 18 | 18 | 4.5[a] | 13.5 |
| 4-Nitro-2-hydroxytoluene | 21 | 11 | 7 | 13.0 |
| 5-Nitro-2-hydroxytoluene | 49 | 29 | 43 | 40.3 |
| 3-Nitro-4-hydroxytoluene | 5 | 26 | 4.5[a] | 11.8 |

[a] Estimate, unable to resolve gas chromatographic peaks.

sample exceeded the amount of benzaldehyde reacted. Thus, although benzoic acid production may have occurred in the gas phase, this was probably masked by heterogenous processes within the collected sample involving unreacted benzaldehyde. Also detected were *p*-benzoquinone and two other unknown minor products. Analysis of benzaldehyde filter samples indicates that no aerosol products formed in the absence of HONO, and only two products formed in the HONO/$h\nu$ experiments. The major aerosol species detected was identified by GCMS as *p*-nitrophenol. Benzoic acid was not detected in any filter extractions.

Batch photolysis experiments were performed with HONO for all cresols, *m*-nitrotoluene, and methyl-*p*-benzoquinone (also performed without HONO). Both the *o*-cresol and *p*-cresol systems developed gas-phase products. These were identified as 3-nitro-2-hydroxytoluene, 5-nitro-2-hydroxytoluene (from *o*-cresol), and 3-nitro-4-hydroxytoluene (from *p*-cresol). No high-molecular-weight products were found for the *m*-cresol, *m*-nitrotoluene, or methyl-*p*-benzoquinone batch systems.

## Discussion

### *Initial Reactions*

The hydroxyl radical reacts with toluene in two ways: methyl hydrogen abstraction or $HO^{\cdot}$ addition to the aromatic ring.

(3)

(4)

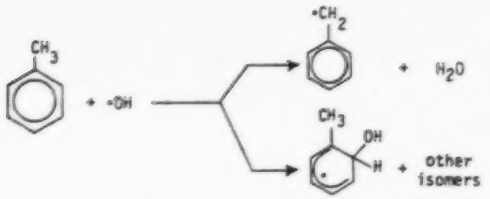


A complete HO·-toluene reaction scheme is shown in Figure 2 and explained below.

*Abstraction Pathway*

After HO· abstracts a methyl hydrogen to form benzyl radical [reaction (3)], oxygen adds to the radical carbon, yielding a benzylperoxy radical. The formation of benzaldehyde occurs by the subsequent reaction of this species [5,11,18,38]:

(5) $$C_6H_5CH_2OO\cdot + NO \longrightarrow C_6H_5CH_2O\cdot + NO_2$$

(6) $$C_6H_5CH_2O\cdot + O_2 \longrightarrow C_6H_5CHO + HO_2\cdot$$

These oxygenated radicals may also react to form benzyl nitrate and benzyl nitrite through the reactions shown below:

(7) $$C_6H_5CH_2OO\cdot + NO \longrightarrow C_6H_5CH_2ONO_2$$

(8) $$C_6H_5CH_2O\cdot + NO_2 \longrightarrow C_6H_5CH_2ONO_2$$

(9) $$C_6H_5CH_2O\cdot + NO \longrightarrow C_6H_5CH_2ONO$$

In the toluene/HONO/$h\nu$ CSTR experiments of 18- to 23-min residence time (experiments 3–7), benzaldehyde yields averaged 10.4 ± 2.9% (associated error values are two standard deviations plus experimental error when applicable). These results fall between the experimental yields of Atkinson, Carter, and Winer [13] (7.3 ± 2.2%), and the low-pressure data of Kenley, Davenport, and Hendry [11] (15 ± 2%). Benzyl nitrate yields were only 0.7 ± 0.4% of the reacted carbon (about 7% of benzaldehyde yields) even though $NO_x$ concentrations were higher than ambient levels. Hoshino, Akimoto, and Okuda [10] found benzyl nitrate concentrations to be 12 ± 4% of benzaldehyde yields. Both results indicate that this process is relatively unimportant, either because the rates of reaction are slow, or because benzyl nitrate photolysis (to the original reactants [39]) is rapid. Reaction (9) is probably unimportant since benzyl nitrite should readily photolyze [38,39].

Given the amounts of toluene reacted and benzaldehyde and benzyl nitrate formed in each experiment, it is possible to estimate the

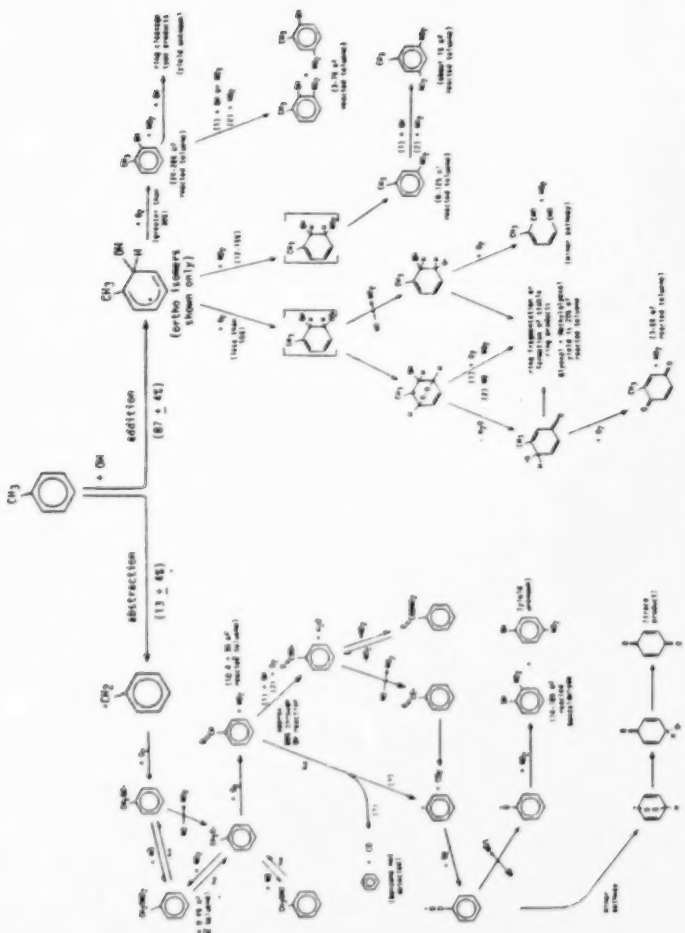

Figure 2. Hydroxyl radical-toluene reaction scheme for the CSTR experiments. Notes: (a) Recall that [NO] and [$NO_2$] were high in these experiments. Lower values in the atmosphere limit the importance of the + NO and + $NO_2$ reaction pathways. (b) All yields are molar. (c) Major isomers are used to represent all possible isomers. (d) Percent yields are for all isomers even if only one shown. See text for isomeric ratios.

amount of methyl hydrogen abstraction by assuming that these species and benzaldehyde oxidation products represent the carbon of the abstraction pathway. The products of benzaldehyde oxidation result mainly from photolysis and reaction with hydroxyl radical [18,38]. Reaction with $NO_3^\cdot$ is too slow to be significant [9], while the low CSTR concentrations of $O_2$ and $HO_2^\cdot$ (calculated) prohibit possible reaction with these species. The rate constant for the reaction of $O^{3P}$ with benzaldehyde (by analogy with $O^{3P}$-aliphatic aldehyde rates) could be high enough to slightly influence the loss of benzaldehyde but should not cause significant error in the abstraction yield calculations if it is neglected.

Using benzaldehyde yields, $HO^\cdot$ concentrations estimated from chemical kinetics modeling of each experiment, and photolysis and $HO^\cdot$ reaction rates (below and in refs. [18] and [38]), calculations showed that the experimental yields of benzaldehyde represented about 80% of the carbon that reacted to become benzaldehyde during the CSTR residence time. Also, the total mass of benzaldehyde and its reaction products accounted for approximately 80–90% of the carbon that passed through the abstraction pathway.

Once the abstraction pathway yield was estimated, the ratio of abstraction to addition could be calculated by first accounting for the small amount of $O^{3P}$ oxidation in the remaining reacted toluene (less than 0.5%) and assuming the difference represented the amount of $HO^\cdot$ addition to toluene. Performing these calculations for each experiment, the best value of $[k_3/(k_3 + k_4)]$ in these data was 0.13 ± 0.04. This can be compared to previous results from Perry, Atkinson, and Pitts [40] ($0.16^{+0.07}_{-0.05}$), Kenley, Davenport, and Hendry [11] (0.15 ± 0.02), and Atkinson, Carter, and Winer [13] (0.08 ± 0.03).

The processes by which benzaldehyde photolyzes in the atmosphere are unclear [38]. In this study it was assumed that benzaldehyde probably formed stable species such as benzene and carbon monoxide [41], although significant yields of benzene were not found in the CSTR photolysis experiments. This agreed with the experience of Atkinson and co-workers [18], who found it necessary to model benzaldehyde photolysis on toluene smog chamber experiments with nonradical products but could not account for large predicted benzene concentrations with the experimental yields. Conversely, Killus and Whitten [30] assumed photolytic production of phenyl radical, $HO_2^\cdot$ and CO but at a lower photolytic rate. Table III contains results from two benzaldehyde photolysis experiments. An average maximum loss rate of $1.1 \pm 0.4 \times 10^{-3}$ $min^{-1}$ was calculated. This value is about 60–70% of rates that have been estimated in the photochemical kinetics simulation models with stable products [18,29] and almost identical to the value used by Killus and Whitten [30] when assuming radical products.

TABLE III. Kinetic data from benzaldehyde photolysis experiments in the CSTR.

| | Conditions | |
|---|---|---|
| Experiment Number | 8 | 9 |
| Residence Time (min.) | 22.41 | 22.93 |
| Dark Exit Concentration (ppmC) | 17.13 | 18.22 |
| Lights-on Exit Concentration (ppmC) | 16.71 | 17.78 |
| Δ [benzaldehyde] (ppmC) | 0.42 | 0.44 |
| Δ [benzaldehyde] (percent) | 2.45 | 2.41 |
| Temperature (Kelvin) | 302.6 | 299.0 |
| Benzaldehyde Loss Rate ($min^{-1}$) | $1.09 \times 10^{-2}$ | $1.05 \times 10^{-2}$ |

Because of the high reaction rate of $HO^{\cdot}$ with benzaldehyde [42,43], this process predominates over photolysis loss in the CSTR (this ratio is estimated to be ca. 5 or 6 to 1). The high reaction rate also indicates that reaction occurs primarily through $HO^{\cdot}$ abstraction of the aldehydic hydrogen [18,38], rather than through $HO^{\cdot}$ addition to the aromatic ring. This conclusion is supported by the lack of ring-decomposition products such as glyoxal and methylglyoxal in any benzaldehyde/HONO/$h\nu$ experiment. These product species occur when the aromatic ring is cleaved upon $HO^{\cdot}$ addition to toluene and xylene rings [20,24,25,44].

After aldehydic H abstraction from benzaldehyde, oxygen adds to the benzoyl radical to form the peroxybenzoyl radical, which reacts with both NO or $NO_2$ as shown below [19,45–47]:

(10) $$C_6H_5C(O)OO^{\cdot} + NO_2 \rightleftharpoons C_6H_5C(O)OONO_2$$

(11) $$C_6H_5C(O)OO^{\cdot} + NO \longrightarrow C_6H_5C(O)O^{\cdot} + NO_2$$

Measurements of peroxybenzoyl nitrate (PBzN) concentration were not taken in any experiment; therefore, it is possible that a large fraction of reacted benzaldehyde carbon may have gone undetected as PBzN. It has been shown [19,46], however, that NO effectively competes with $NO_2$ for reaction with the peroxybenzoyl radical [reaction (11)]. Using the rates of Kenley and Hendry [46], computer simulations of the CSTR chemistry indicate that PBzN yields would have been in the order of 0.5% of reacted toluene carbon.

Niki et al. [19] proposed further reactions, consistent with their data, as shown below:

(12) $$C_6H_5C(O)O^{\cdot} \longrightarrow C_6H_5^{\cdot} + CO_2$$

(13) $$C_6H_5^{\cdot} + O_2 \longrightarrow C_6H_5OO^{\cdot}$$

(14) $$C_6H_5OO^{\cdot} + NO \longrightarrow C_6H_5O^{\cdot} + NO_2$$

(15) $$C_6H_5O^{\cdot} + NO_2 \longrightarrow (o\text{- and } p\text{-})C_6H_4(OH)NO_2$$

*o*-Nitrophenol was detected in the gas phase for CSTR HONO/$h\nu$ experiments of both benzaldehyde and toluene. *p*-Nitrophenol occurred

as aerosol in the benzaldehyde CSTR system. These results verify the Fourier transform infrared spectroscopic identification of gas-phase *o*-nitrophenol and tentative identification of condensed phase *p*-nitrophenol by Niki et al. [19]. Approximately 14–18% of the reacted benzaldehyde molecules could be accounted for as *o*-nitrophenol after 21 min. The yield of aerosol *p*-nitrophenol was not quantified, although the amount detected on the GCMS system was significant. Thus, evidence indicates that nitrophenol formation is a major process in benzaldehyde oxidation, although the existence of an alternate pathway cannot be ruled out because the *p*-nitrophenol yield was unquantified.

Two other gas-phase products, *p*-benzoquinone (trace) and an unidentified compound (estimated 2–5% yield) also were detected. The *p*-benzoquinone may have formed from phenylperoxy radical in a manner analogous to that proposed for methyl-*p*-benzoquinone (see below). In addition, phenol was not detected in any toluene or benzaldehyde experiments, indicating that the alternate reaction scheme:

(16) $$C_6H_5O^{\cdot} + HO_2^{\cdot} \longrightarrow C_6H_5OH + O_2$$

was unimportant in the CSTR experiments.

*Addition Pathway*

The hydroxyl radical can add to the toluene ring in one of four positions. Addition to the 1-position should entail displacement of the methyl group and formation of phenol [5]. Because phenol was not detected, this process is thought to be unimportant. Evidence for *o*-, *m*-, and *p*-hydroxytoluene adducts does exist, however, in the formation of cresol and nitrotoluene isomers.

After addition of $HO^{\cdot}$ [reaction (4)], $NO_2$ can add to the radical ring, later regenerating the aromatic structure by losing water and forming a nitrotoluene isomer [18,48]. The case for the ortho $HO^{\cdot}$-adduct is shown below:

(17)

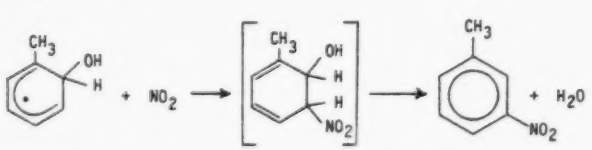


Assuming $NO_2$ addition to the 1-position is sterically limited, $HO^{\cdot}$-toluene adduct resonance structures predict the formation of only *m*-nitrotoluene for ortho and para $HO^{\cdot}$-adducts and either *o*- or *p*-nitrotoluene for the meta $HO^{\cdot}$-adduct. Since $NO_2$ concentration was higher in the CSTR than in the atmosphere, and because it is an effective radical terminator, processes involving $NO_2$ [such as reaction (17)] were more significant in the CSTR. Hence, larger

amounts of measurable products were detected, allowing calculation of more precise isomeric product ratios and rates of reaction.

Further reaction of nitrotoluenes might occur through another $HO^{\cdot}$ attack on the aromatic ring. Results from *m*-nitrotoluene/HONO/$h\nu$ batch experiments indicated that that system did not yield detectable amounts of nitrocresol species. 3,5-Dinitrotoluene, however, was identified as a significant aerosol product in toluene CSTR experiments (Table II), possibly forming from *m*-nitrotoluene in a manner analogous to reaction (17). Isomeric fractions, including aerosol nitrotoluenes and 3,5-dinitrotoluene (contained in the *m*-nitrotoluene yield), are given for each CSTR experiment in Table IV. The average fractions were $o/m/p \approx 7/74/19$ for experiment 3 through 7 (residence times near 20 min) and $o/m/p \approx 7/72/21$ for all experiments. Assuming the mechanism of reaction (17) is resonance structure exclusive, these yields indicate that nitrotoluenes from $HO^{\cdot}$ attack at the meta position account for about 27% of the nitrotoluene detected, with the ortho or para $HO^{\cdot}$-adducts accounting for the remaining 73% (*m*-nitrotoluene). In addition, the ratio of *p*- to *o*-nitrotoluene was about 3:1, probably indicating the steric effect of the methyl group upon $NO_2$ approach to the meta $HO^{\cdot}$-adduct. Comparison with earlier results is difficult since only this study has detected aerosol products and consistently measured *o*-nitrotoluene. Although searched for, *o*- and *p*-nitrotoluene isomers were not detected by Kenley, Davenport, and Hendry [11], even though *m*-nitrotoluene averaged over 30% of detected products. Hoshino, Akimoto, and Okuda [10] found *p*-nitrotoluene to account for about one-third of the nitrotoluene yield, with *m*-nitrotoluene becoming more dominant as $NO_x$ was increased. This trend is not apparent in Tables I and IV.

Besides addition of $NO_2$, the $HO^{\cdot}$ addition products can regenerate aromatic structure by displacing hydrogen to form $HO_2^{\cdot}$ and corresponding cresols [10,12]:

(18)

Results from toluene CSTR and cresol batch experiments indicate that cresols reacted further in the HONO/$h\nu$ system to form nitrocresols. Condensed phase hydroxynitrocresols, identified by Grosjean et al. [17], were not detected in any experiments; possibly because of the shorter CSTR residence time. From the batch experiments it was found that each cresol isomer produced only nitrocresol species with methyl-to-hydroxyl orientation identical to the parent cresol. Hence, it was possible to attribute the formation of nitrocresol products in the toluene/HONO/$h\nu$ experiments to the appropriate sites of initial

TABLE IV. Selected ratios for toluene CSTR experiments.

| Experiment Number | 1 | 2 | 3 | 4 | 5[a] | 6 | 7 | | |
|---|---|---|---|---|---|---|---|---|---|
| Residence Time (min.) | 8.35 | 12.51 | 16.35 | 21.45 | 21.47 | 22.08 | 22.66 | | |
| Δ[toluene] (ppmC) | 3.47 | 4.83 | 11.77 | 5.44 | 8.37[a] | 8.08 | 7.85 | | |
| Δ[toluene] (percent) | 2.06 | 5.49 | 6.88 | 6.19 | 6.15[a] | 7.28 | 7.05 | | |
| Inlet [$NO_x$] (ppm) | n.a. | 4.5 | 19.3 | 6.6 | 20.1 | 10[a] | 6.4 | | |
| [HC]/[$NO_x$] (ppmC/ppm) | n.a. | 19.5 | 8.9 | 13.3 | 8.8[a] | 11.1[a] | 15.5 | | |
| **Product Ratios** | | | | | | | | | |
| | | | | | | | | Averages ± 2 s.d. All | Averages ± 2 s.d. ≈ 20 min. |
| DICARBONYLS: | | | | | | | | | |
| [GLY]/[MGLY] (carbon) | 0.75 | 0.56 | 0.57 | 0.70 | 0.67 | 0.60 | 0.64 | 0.65 ± 0.14 | 0.65 ± 0.10 |
| [GLY]/[MGLY] (molar) | 1.13 | 0.84 | 0.86 | 1.05 | 1.00 | 1.04 | 0.96 | 0.98 ± 0.21 | 0.98 ± 0.15 |
| NITROTOLUENES: | | | | | | | | | |
| ortho | 8.9 | 7.8 | 5.9 | 5.8 | | 8.5a | 6.8 | 7.2 ± 2.5 | 6.7 ± 2.2 |
| meta | 67.1 | 69.2 | 78.4 | 73.9 | | 72.9 | 71.1 | 72.1 ± 7.2 | 74.1 ± 5.4 |
| para | 24.0 | 23.0 | 15.7 | 20.5 | | 18.6 | 22.1 | 20.6 ± 5.6 | 19.2 ± 4.7 |
| TOTAL CRESOLS: | | | | | | | | | |
| ortho | 71.4 | 81.9 | 83.2 | 84.0 | | 80.7 | 83.2 | 80.7 ± 8.6 | 82.6 ± 2.5 |
| meta | 4.6 | 2.6 | 1.1 | 2.3 | | 2.1 | 2.2 | 2.5 ± 2.1 | 1.9 ± 0.9 |
| para | 24.0 | 15.5 | 15.7 | 13.7 | | 17.2 | 14.6 | 16.8 ± 6.8 | 15.3 ± 2.6 |
| OTHER RATIOS: | | | | | | | | | |
| Σ Cresols/Benzaldehyde | 2.57 | 3.73 | 2.12 | 2.57 | | 2.54 | 3.26 | 2.80 ± 1.07 | 2.62 ± 0.82 |
| o-Cresol/Benzaldehyde | 1.83 | 3.05 | 1.76 | 2.16 | | 2.05 | 2.72 | 2.26 ± 0.94 | 2.17 ± 0.69 |

[a]Gas chromatograph calibrations not available for this experiment. Data not included in table.
[a]Estimated.

$HO^{\cdot}$ addition (Table I). The mechanism by which this occurs, however, is not clear. Rates of reaction for $HO^{\cdot}$ with cresols [26] and $NO_3$ with cresols [9] indicate that these processes alone cannot contribute enough mass to account for the gas-phase nitrocresol yields. Possible mechanisms by which additional cresol-to-nitrocresol conversion could occur include: (1) unidentified gas-phase reactions (possibly between HONO and cresol), (2) heterogeneous surface reactions in the CSTR, and (3) nitration of cresols during sample concentration prior to GC injection. Although sample concentration lasted for only about 2 min at −77°C, such reactions for cresols have been suggested [10,11,15]. For modeling purposes, we assumed that all species identified as gas-phase nitrocresols were cresols [10] (probably overestimating cresol concentration slightly) and nitrocresols measured on filter samples represented actual condensed-phase nitrocresols. Using this assumption, the gas-phase *o*-cresol yield averaged about 22% (Table I). This was larger than the yield of Atkinson, Carter, and Winer [13] (13.1 ± 7.2%) but equal to the rate constant fraction needed by Atkinson and co-workers to model toluene smog chamber experiments [18].

By assuming that 65% of filter mass was due to nitro-*o*-cresols and 15% to 3-nitro-4-hydroxytoluene (Table II), the amounts of cresol products (cresol + nitrocresols) that resulted from $HO^{\cdot}$ attack at different sites of the toluene ring could be estimated. Results given in Table IV indicate that the average isomeric ratios were approximately $o/m/p = 82/2/16$ for experiments 3–7 (about 20-min residence time) and $o/m/p \approx 80/2/17$ for all experiments. This agrees with the previous estimates of Hoshini, Akimoto, and Okuda [10] ($o/(m + p) \approx 80/20$) and Kenley, Davenport, and Hendry [11] ($o/m/p \approx 75/11/14$). The disparity between the meta fraction of this study and that of Kenley and co-workers may be due to undetected CSTR nitro-*m*-cresol species, artificially enhancing the ortho and para fractions. However, given the range of chromatographic techniques used on both toluene/HONO/$h\nu$ CSTR and *m*-cresol/HONO/$h\nu$ batch experiments, it is far more likely that any nitro-*m*-cresol products were not detected because they occurred at concentrations below the chromatographic sensitivity for these species. At most this could alter the isomeric fractions by only a few percent.

An alternate explanation is that although a larger percentage of meta $HO^{\cdot}$ addition occurred, very little *m*-cresol formed in the CSTR experiments. Recall that 27% of the nitrotoluene yield was expected to originate from meta $HO^{\cdot}$-adduct reactions. Therefore, it is possible that the meta $HO^{\cdot}$-adduct, compared to the ortho and para isomers, is more likely to form nitrotoluene products under CSTR conditions. This could be due to the meta orientation of the methyl and hydroxyl groups. On aromatic rings this orientation tends to reinforce the electron donating influences of these groups, resulting in ring activation

for electrophilic substitution at the positions ortho and para to those groups [49]. However, whether the reason for the difference in product yields is a comparatively larger rate of reaction with $NO_2$, a slower rate of *m*-cresol formation or the existence of undetermined reaction steps is not known. In the low-pressure discharge flow reactor of Kenley, Davenport, and Hendry [11], such a difference in the chemistry of these isomers may not have been obvious, since the only identified reaction product of the meta HO·-adduct was *m*-cresol. (It is shown below that use of both nitrotoluene and cresol data to approximate the initial HO· attack sites yields nearly identical results between studies.)

Assuming that products derive only from reaction at resonance structure radical sites, the ratio of $k_{17}/k_{18}$ can be estimated for the ortho and para HO·-adducts (combined since they both form *m*-nitrotoluene) by

$$\frac{k_{17}}{k_{18}} = \frac{[m\text{-nitrotoluenes}]}{[o\text{-cresols}] + [p\text{-cresols}]} \times \frac{[O_2]}{[NO_2]} \tag{19}$$

The similar expression for the meta HO·-adduct is

$$\frac{k_{17}}{k_{18}} = \frac{[o\text{-nitrotoluene}] + [p\text{-nitrotoluene}]}{[m\text{-cresol}]} \times \frac{[O_2]}{[NO_2]} \tag{20}$$

Averaged over all experiments, the former value is approximately $2.5 \times 10^4$, while the latter is estimated to be nearly a factor of 20 larger (with a large associated error, since [*m*-cresol] is a small value of relatively poor precision). Earlier work by Kenley, Davenport, and Hendry [11] set $k_{17}/k_{18}$ at $4 \pm 2 \times 10^3$. Atkinson and co-workers, however, suggested that a value of $k_{17}$ approximately ten times greater than arrived at by using this ratio could more accurately simulate results from toluene smog chamber experiments [18]. The lumped value of $k_{17}/k_{18}$ ($\Sigma$[nitrotoluenes]/$\Sigma$[cresols] × $[O_2]/[NO_2]$) derived from toluene CSTR experiments is about $3.3 \times 10^4$, more in agreement with the estimates of Atkinson. The $NO_2$ concentration in these CSTR experiments averaged about 3 ppm. Therefore, the above calculations indicate that the relative yield of nitrotoluenes to cresols over the range of 0.03 to 0.3 ppm of $NO_2$ would be only about 0.5 to 5%.

The third primary reaction of the HO·-toluene adduct is thought to be the reversible addition of an oxygen molecule [18,38]. In this case, however, more than one isomer can be formed, since the original radical location would have been delocalized across the ring. For the ortho HO·-toluene adduct:

(21)

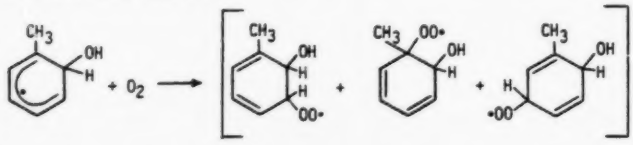

the relative importance of each structure is not known. Atkinson and co-workers [18,38], however, have pointed out that addition to the 5-position is not thermodynamically favored; and addition at the 1-position, while slightly more energetically favored than the 3-position $O_2$ adduct, may be sterically hindered.

To estimate the importance of this process in the CSTR, we use the assumption that reaction (21) accounts for all HO·-adduct carbon not reacting to form measured nitrotoluenes or cresols. A ratio similar to those above may then be defined as

$$(22) \qquad \frac{k_{18}}{k_{21}^{eff}} \geq \frac{\Sigma[\text{cresols}]}{(0.86 \times [\Delta\text{toluene}]) - (\Sigma[\text{cresols}] + \Sigma[\text{nitrotoluenes}])}$$

The HO·-adduct carbon is accounted for in the denominator by subtracting the detected nitrotoluene and cresol yields from 86% of the reacted toluene. The missing 14% of the original toluene carbon is assumed to have reacted through the HO· abstraction pathway (13.2%) along with some loss due to $O^{3}P$ reaction (about 0.5%). Equation (22) is shown as a possible inequality since the right side probably overestimates $k_{18}/k_{21}^{eff}$ because all undetected product mass, including cresol reaction products that were not nitrocresols, is included in the [Δtoluene] term. Using all available CSTR data, the average value of $k_{18}/k_{21}^{eff}$ was determined to be $\geq 0.6 \pm 0.3$. The effect of lower $NO_2$ concentrations was estimated by replacing the Σ[nitrotoluenes] term with $k_{17}/k_{18} \times [NO_2]/[O_2] \times \Sigma[\text{cresols}]$ [from the lumping of eqs. (19) and (20)]. Calculations show that as $[NO_2]$ drops below about 0.2 ppm, this lumped term becomes insignificant, resulting in $k_{18}/k_{21}^{eff} \geq 0.5 \pm 0.2$ as the limit when $[NO_2]$ approaches zero. The values of this ratio in published toluene models are 0.20 [29], 0.31 [28], 0.34 [18], and 0.35 [30]. These estimates appear to be lower than that calculated, although the higher values are within the associated error bands. The effect of too low a value within a model would be to route extra mass through the $O_2$-adduct pathway at the expense of cresol product species.

It has been proposed that toluene $O_2$-adduct radicals undergo cyclization by creating $O_2$ bridges across the ring; although there is disagreement as to the orientation of this structure and the subsequent reaction mechanism [18,20,38,50,51]. Continuing with the ortho HO·-adduct example:

(23)

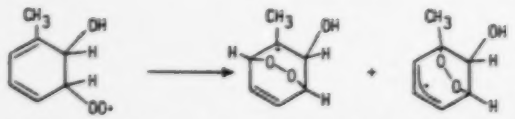


Results from this study provide evidence for the existence of the [2.2.2] bicyclic radical. Formation of methyl-*p*-benzoquinone, through

loss of water and cleavage of the oxygen bridge, followed by formation of a stable quinoid structure by loss of $HO_2^{\cdot}$, is shown below.

(24)

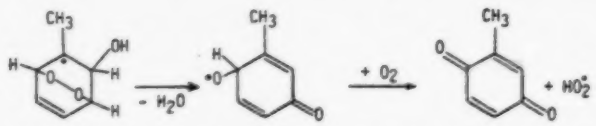

The reaction might occur more readily for the ortho isomer shown above, since the radical is tertiary and the final formation of methyl-*p*-benzoquinone requires severing of a C—H bond. In the case of the meta $HO^{\cdot}$-adduct, cleavage of the C—$CH_3$ bond would be required to form *p*-benzoquinone (not detected in toluene CSTR experiments). Recall, however, that traces of *p*-benzoquinone were formed as a product of benzaldehyde photooxidation experiments. Bridging of $O_2$ across the phenylperoxy radical to form a bicyclic radical by a process similar to that above may be envisioned

(25)

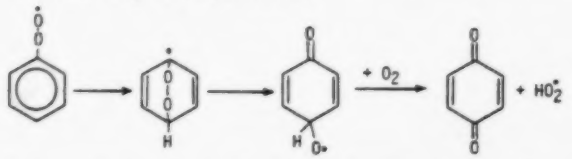

Methyl-*p*-benzoquinone has also been identified as a minor product (<1%) by Kenley, Davenport, and Hendry [11], and detected in UNC outdoor smog chamber experiments with toluene and $NO_x$. Dimethyl-*p*-benzoquinones occur in comparable yields for xylene/HONO/$h\nu$ CSTR experiments [44] and smog chamber systems [52]. The atmospheric chemistry of these species is not known, although the structure of this compound (conjugated carbonyl and olefin bonds) suggests some atmospheric photooxidation is likely by analogy with similar species. Reaction in batch photolysis experiments did occur, although the rate was not determined. No products, including dicarbonyl species, were detected in either $h\nu$ or HONO/$h\nu$ batch experiments.

Besides forming quinones, bicyclic radicals may react further, eventually resulting in ring cleavage and formation of some stable oxygenated species. Atkinson and Lloyd have presented an analysis of possible reaction schemes and chemical kinetics for suspected fragmentation processes [38]. The most prominent products are glyoxal and methylglyoxal [20,21,23–25] (and possibly CO, $CO_2$, and formaldehyde). In this study, glyoxal and methylglyoxal molar yields, corrected for $HO^{\cdot}$ reaction and photolysis losses [27] and averaged over all experiments, were 9.8 and 10.6%, respectively. The mean ratio of glyoxal to methylglyoxal was 0.94 ± 0.19 molecule/molecule, similar to those of other studies (0.76 [24] and 1.07 [20,25]). In terms of reacted toluene carbon, the corrected combined yield of glyoxal and

methylglyoxal averaged 7.3%, while yields from other work were 5.5 [20], 9.5 [24], and 10.3 [25] % of reacted carbon. Comparison of the glyoxal and methylglyoxal carbon yields from toluene CSTR experiments with results from xylene systems of similar $NO_x$ and residence times [44] indicates that toluene yields were approximately 40% of *m*-xylene yields and 30% of those from *o*-xylene (including biacetyl in the *o*-xylene yields). Again, these relative yields compare favorably with trends from other studies [20,24,25].

Although oxygenation and ring cleavage are prerequisites for formation of dicarbonyl products, the reactions through which ring decomposition occurs are not verified. Various competitive processes could result in different product distributions as the structural and energetic characteristics of the reacting ring species are varied. As noted above, dicarbonyl yields for toluene are considerably lower than those of xylene systems. This may indicate that the degree of benzene ring methylation influences the yield of dicarbonyl species. Additional methyl groups could result in higher $k_{*ff}$ for reaction (21) through stabilization of the $O_2$-adduct radical (lessening $k_{-21}$). In addition, steric hinderance could yield higher rates of intramolecular reaction (ring decomposition and quinone formation through peroxide bridging). The relative orientation of methyl groups might also influence the transition state energy of decomposing reactants and definitely leads to different product distributions, which can influence system reactivity. Clearly, however, if these trends exist, they have only been demonstrated over a small range. To explore this process further, dicarbonyl yields from similar species must be obtained, including isomers with larger alkyl groups of both electron donating and steric shielding effects.

The combined molar yields of glyoxal and methylglyoxal in the other studies discussed above range from 15.5 [20] to 25.7 [24] and 29 [25]%. The value in this study is about 20%. Shepson, Edney, and Corse [20] identified an additional 3.6-mol.% yield as longer-chain, conjugated, oxygenated fragmentation products. However, even if it is assumed that every dicarbonyl species represents one fragmented ring, the above yields account for only about half of the HO·-adduct molecules expected to pass through reaction (21) [from eq. (22), if $k_{18}/k_{21}^{eff} \approx 0.6$ and nitrotoluene formation is minimal, approximately 60% of the HO·-adducts should react through $O_2$ addition). Thus, results from this and other studies indicate that a significant amount of the molecules expected to pass through reaction (21) do not yield dicarbonyl products. Whether the missing products are non-dicarbonyl fragmentation species (a small percentage of the reacted carbon is probably CO, $CO_2$, and formaldehyde) or stable compounds formed prior to ring cleavage is not clear.

Compared with reactions (17) and (18), reaction (21) involves extra reaction steps prior to formation of most of the fragmentation

products detected. Because of these extra reactions and the various isomeric products in each, the many low-yield pathways could accumulate a significant portion of the reacted carbon as undetected products. Hoshino, Akimoto, and Okuda [10] tentatively identified 2-methyl-2,4-hexadienedial as a minor product, possibly resulting from reaction (26)

(26) 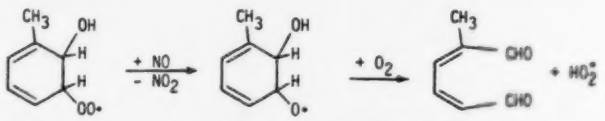


and Kenley, Davenport, and Hendry [11] detected traces of methyl-*p*-benzoquinone. Because product yields were low, however, photochemical kinetics models have ignored these reactions in favor of rapid ring decomposition. The measurement of 3–6% methyl-*p*-benzoquinone yields in this study indicates that ring fragmentation is not instantaneous, and that the $O_2$-adduct or the [2.2.2] bicyclic radical may be somewhat stable. Thus, to more accurately describe the complex $O_2$-adduct reaction scheme, photochemical kinetics models may need to consider additional prefragmentation reaction steps. Besides further reactions of methyl-*p*-benzoquinone, some possible reactions of the $O_2$-adduct and subsequent species, involving NO-to-$NO_2$ conversion and formation of organic and organic nitrate products have been proposed [10,18,38]. Significant reaction in these pathways will limit the molecules available for rapid ring decomposition schemes, and could also be difficult to detect because of the low yields of many products with unknown molecular structures.

Finally, it is possible to estimate the relative fractions of initial $HO^{\cdot}$ addition sites on the toluene aromatic ring by employing the method of Kenley, Davenport, and Hendry [11].

(27)
$$f_{\text{ortho}} = \frac{\left(\left(\frac{[o\text{-cresols}]}{([o\text{-cresols}]+[p\text{-cresols}])}\right)\times[m\text{-nitrotoluenes}]\right)+[o\text{-cresols}]}{\Sigma[\text{cresols}]+\Sigma[\text{nitrotoluenes}]}$$

(28)
$$f_{\text{meta}} = \frac{[m\text{-cresol}] + [o\text{-nitrotoluene}] + [p\text{-nitrotoluene}]}{\Sigma[\text{cresols}] + \Sigma[\text{nitrotoluenes}]}$$

(29)
$$f_{\text{para}} = \frac{\left(\left(\frac{[p\text{-cresols}]}{([o\text{-cresols}]+[p\text{-cresols}])}\right)\times[m\text{-nitrotoluenes}]\right)+[p\text{-cresols}]}{\Sigma[\text{cresols}]+\Sigma[\text{nitrotoluenes}]}$$

This approximation, however, is based on the yields of identified cresol and nitrotoluene products only and, thus, must assume that the

results are representative of the $O_2$ addition pathway. Since that reaction is probably the most significant HO·-adduct reaction, these values can only be used as a first approximation. Averaged over the longer residence time experiments, this ratio is $f_{ortho}/f_{meta}/f_{para} \approx$ 78/8/14 (averaged for all experiments ≈ 75/9/16). Kenley, Davenport, and Hendry [11] found this ratio to be 81/5/14.

## Conclusions

In this study, 55–75% of the reacted carbon from the HO·-toluene reaction was accounted for in both gas-phase and aerosol products. Because of these high CSTR yields at atmospheric pressure, more precise calculation of the mass flow through various reaction schemes could be established compared with earlier studies. Approximately 13% of the original oxidation occurred through methyl H· abstraction by HO·; primarily leading to benzyl nitrate, benzaldehyde, and subsequent reaction products. Gas-phase *o*-nitrophenol and condensed *p*-nitrophenol were major products from the HO·-benzaldehyde reaction, but no products were detected in the photolysis of benzaldehyde. The remaining 87% of the original oxidation was expected to react through the addition pathway; producing cresols, nitrocresols, nitrotoluenes, 3,5-dinitrotoluene, methyl-*p*-benzoquinone, methylglyoxal, and glyoxal.

Yields of cresols and nitrotoluenes were used to calculate the reaction rate constant ratio between HO·-adduct reactions with $NO_2$ and $O_2$ (to form cresol). The value of $k_{17}/k_{18}$ was determined to be about $3.3 \times 10^4$, producing a higher reaction rate with $NO_2$ than had been reported earlier, but still indicating that this reaction accounts for very little of the HO·-adduct carbon (probably less than 5% under atmospheric conditions). The cresol formation pathway, however, was found to be much more significant than previously expected. Data in this study indicate that some of the reacted toluene carbon undetected in earlier work may have been unmeasured cresol products rather than $O_2$ addition products. From these data the ratio of HO·-adduct rate constants for cresol formation versus $O_2$ addition ($k_{18}/k_{21}^{eff}$) is calculated to be ≥0.6. This implies that at least 35% of the addition pathway carbon is accounted for in cresol formation. This value is at least twice as high as earlier photochemical kinetics model estimates. Clearly, more work is needed to establish this ratio accurately; however, the estimate does indicate the need for further experimental investigation of the chemistry of cresols. *o*-Cresol, the most prominent isomer, should be studied not only with regards to atmospheric reaction schemes similar to those of toluene, but also, with consideration given to reactions of the phenol group and its effect upon ring fragmentation and aerosol formation processes.

Known ring-fragmentation products, formed from $O_2$ addition to the HO·-toluene adduct, were found to be of yields similar to those of other studies. However, even if it is assumed that each $O_2$-adduct formed only one dicarbonyl compound, the molar yields of these species accounted for only about half of $O_2$-adducts expected to have reacted. Some of the remaining carbon was probably in non-dicarbonyl fragmentation products (other than CO, $CO_2$, and formaldehyde), although the detection of methyl-*p*-benzoquinone indicates that prefragmentation intermediates are stable enough to yield this and possibly other products prior to ring cleavage. Therefore, although it may be possible to represent the $O_2$-adduct reactivity by assuming that all reaction leads to dicarbonyl species, experimental results indicate that this description is not valid in an absolute sense. Various low-yield reactions could account for a large fraction of the undetected carbon. This reaction pathway, because of its complexity, remains the least understood of the HO·-adduct reactions. It is recommended that a CSTR investigation, similar to this one, be undertaken at slightly shorter residence times with more appropriate analytical support to identify additional prefragmentation and fragmentation products formed in the $O_2$-adduct reaction pathway. Also, because of the high methyl-*p*-benzoquinone yields and atmospheric reactivity of species with analogous structures, the chemistry of this product must be investigated and included in photochemical kinetics simulation models.

## Acknowledgments and Disclaimer

We thank Richard Kamens for his many hours of theoretical and analytical discussion, Daryl Sharp for performing GCMS analysis and Jean Perry for providing an array of analytical support. Although the research described in this article has been funded in part by the United States Environmental Protection Agency through cooperative agreements R809954 entitled "Experimental Study of Aerosol Formation Mechanisms in a Controlled Atmosphere," and R808881 entitled "Outdoor Smog Chamber Experiments to Test Photochemical Models," it has not been subjected to the Agency's required peer and policy review and therefore does not necessarily reflect the views of the Agency and no official endorsement should be inferred.

## Bibliography

[1] J. G. Calvert, *Environ. Sci. Technol.*, **10**, 256 (1976).
[2] W. A. Lonneman, S. L. Kopczynski, P. E. Darley, and F. D. Sutterfield, *Environ. Sci. Technol.*, **8**, 229 (1974).
[3] E. S. Jacobs, *Anal. Chem.*, **38**, 43 (1966).

[4] J. B. Maynard and W. N. Sanders, *J. Air Poll. Control Assn.*, **19**, 505 (1969).
[5] R. Atkinson, K. R. Darnall, A. C. Lloyd, A. M. Winer, and J. N. Pitts, Jr., *Adv. Photochem.*, **11**, 375 (1979).
[6] F. P. Tully, A. R. Ravishankara, R. L. Thompson, J. M. Nicovich, R. C. Shah, N. M. Kreutter, and P. H. Wine, *J. Phys. Chem.*, **85**, 2262 (1981).
[7] C. T. Pate, R. Atkinson, and J. N. Pitts, Jr., *J. Environ. Sci. Health*, **A11**, 1 (1976).
[8] R. Atkinson and J. N. Pitts, Jr., *J. Phys. Chem.*, **78**, 1780 (1974).
[9] R. Atkinson, W. P. L. Carter, C. N. Plum, A. M. Winer, and J. N. Pitts, Jr., *Int. J. Chem. Kinet.*, **16**, 887 (1984).
[10] M. Hoshino, H. Akimoto, and M. Okuda, *Bull. Chem. Soc. Jpn.*, **51**, 718 (1978).
[11] R. A. Kenley, J. E. Davenport, and D. G. Hendry, *J. Phys. Chem.*, **85**, 2740 (1981).
[12] H. Akimoto, M. Hoshino, G. Inoue, M. Okuda, and N. Washida, *Bull. Chem. Soc. Jpn.*, **51**, 2496 (1978).
[13] R. Atkinson, W. P. L. Carter, and A. M. Winer, *J. Phys. Chem.*, **87**, 1605 (1983).
[14] C. W. Spicer and P. W. Jones, *J. Air Poll. Control Assoc.*, **27**, 1122 (1977).
[15] D. G. Hendry, in "Chemical Kinetic Data Needs for Modeling the Lower Troposphere," NBS Special Publication No. 557, Washington, DC, 1979.
[16] R. J. O'Brien, P. J. Green, R. A. Doty, J. W. Vanderzanden, R. R. Easton, and R. P. Irwin, in "Nitrogenous Air Pollutants," Ed. D. Grosjean, Ann Arbor Press, Ann Arbor, MI, 1979.
[17] D. Grosjean, *Atmos. Environ.*, **18**, 1641 (1984).
[18] R. Atkinson, W. P. L. Carter, K. R. Darnall, A. M. Winer, and J. N. Pitts, Jr., *Int. J. Chem. Kinet.*, **12**, 779 (1980).
[19] H. Niki, P. D. Maker, C. M. Savage, and L. P. Breitenbach, in "Nitrogeneous Air Pollutants," Ed. D. Grosjean, Ann Arbor Press, Ann Arbor, MI, 1979.
[20] P. B. Shepson, E. O. Edney, and E. W. Corse, *J. Phys. Chem.*, **88**, 4122 (1984).
[21] A. C. Besemer, *Atmos. Environ.*, **16**, 1599, (1982).
[22] R. J. O'Brien, B. E. Dumdei, S. V. Hummel, and R. A. Yost, *Anal. Chem.*, **56**, 1329 (1984).
[23] K. Nojima, K. Fukaya, S. Fukui, and S. Kanno, *Chemosphere*, **3**, 247 (1974).
[24] E. C. Tuazon, R. Atkinson, H. Mac Leod, H. W. Biermann, A. M. Winer, W. P. L. Carter, and J. N. Pitts, Jr., *Environ. Sci. Technol.*, **18**, 981 (1984).
[25] H. Bandow, N. Washida, and H. Akimoto, 11th International Conference on Photochemistry, University of Maryland, College Park, MD, August 21–26, 1983.
[26] R. Atkinson, K. R. Darnall, and J. N. Pitts, Jr., *J. Phys. Chem.*, **82**, 2759 (1978).
[27] C. N. Plum, E. Sanhueza, R. Atkinson, W. P. L. Carter, and J. N. Pitts, Jr., *Environ. Sci. Technol.*, **17**, 479 (1983).
[28] R. Atkinson, A. C. Lloyd, and L. Winges, *Atmos. Environ.*, **16**, 1341 (1982).
[29] J. A. Leone and J. H. Seinfeld, *Int. J. Chem. Kinet.*, **16**, 159 (1984).
[30] J. P. Killus and G. Z. Whitten, *Atmos. Environ.*, **16**, 1973 (1982).
[31] O. Levenspiel, "Chemical Reactor Engineering," Wiley, New York, New York, 1972.
[32] R. A. Cox, *J. Photochem.*, **3**, 175 (1974).
[33] W. H. Chan, R. J. Nordstrom, J. G. Calvert, and J. H. Shaw, *Environ. Sci. Technol.*, **10**, 674 (1976).
[34] J. G. Calvert, "Spectroscopic studies of photochemical smog formation and trace pollutant detection," U. S. Environmental Protection Agency, Research Triangle Park, N. C., Report No. EPA-600/3-76-084 (1976).
[35] R. Kuntz, W. Lonneman, G. Namie, and L. A. Hull, *Anal. Lett.*, **13**, 1409 (1980).
[36] K. Kuwata, M. Uebori, and Y. Yamasaki, *J. Chrom. Sci.*, **17**, 264 (1979).
[37] G. R. Lyles, F. B. Dowling, and V. J. Blanchard, *J. Air Poll. Control Assoc.*, **15**, 106 (1965).
[38] R. Atkinson and A. C. Lloyd, *J. Phys. Chem. Ref. Data*, **13**, 315 (1984).

[39] J. G. Calvert and J. N. Pitts, Jr., "Photochemistry," Wiley, New York, New York, 1966.
[40] R. A. Perry, R. Atkinson, and J. N. Pitts, Jr., *J. Phys. Chem.*, **81**, 296 (1977).
[41] J. R. Majer, S-A. M. A. Naman, and J. C. Robb, *Trans. Faraday Soc.*, **65**, 1846 (1969).
[42] H. Niki, P. D. Maker, C. M. Savage, and L. P. Breitenbach, *J. Phys. Chem.*, **82**, 132 (1978).
[43] J. A. Kerr and D. W. Sheppard, *Environ. Sci. Technol.*, **15**, 960 (1981).
[44] CSTR data to be published for *o*- and *m*-xylene experiments.
[45] B. W. Gay, Jr., R. C. Noonan, J. J. Bufalini, and P. L. Hanst, *Environ. Sci. Technol.*, **10**, 82 (1976).
[46] R. A. Kenley and D. G. Hendry, *J. Am. Chem. Soc.*, **104**, 220 (1982).
[47] T. Ohta and I. Mizoguchi, *Environ. Sci. Technol.*, **15**, 1229 (1981).
[48] E. Halfpenny and P. L. Robinson, *J. Chem. Soc.*, 939, (1952).
[49] F. A. Carey and R. J. Sundberg, "Advanced Organic Chemistry," Plenum, New York, 1977.
[50] K. R. Darnall, R. Atkinson, and J. N. Pitts, Jr., *J. Phys. Chem.*, **83**, 1943 (1979).
[51] J. P. Killus and G. Z. Whitten, *Atmos. Environ.*, **17**, 1597 (1983).
[52] Unpublished data from the UNC outdoor smog chamber.

Received December 3, 1984
Accepted March 1, 1985

NOTICE

This document has been reviewed in accordance with U.S. Environmental Protection Agency policy and approved for publication. Mention of trade names or commercial products does not constitute endorsement or recommendation for use.

This article documents research that was conducted under the auspices of the U.S. Environmental Protection Agency (USEPA). As an arm of the government, the USEPA has a paid up, non-exclusive, irrevocable, worldwide license to reproduce, prepare derivative works, and distribute to the public all of the material contained herein, and to grant others acting on its behalf the right to do so. The USEPA grants to the National Technical Information Service, Department of Commerce, the right to act as its agent in the distribution of this material.